Characterization of the Viscoelastic and Mechanical Properties of Tightly Cross-Linked Polythiourethane Networks

Nicolas Droger,[1,2] Odile Primel,[2] Jean Louis Halary[1]

[1]*ESPCI, Laboratoire PPMD (UMR 7615), 10 rue Vauquelin, 75231 Paris Cedex 05, France*
[2]*Essilor International, Centre Technique, 57 avenue de Condé, 94106 Saint-Maur Cedex, France*

Received 20 December 2006; accepted 6 July 2007
DOI 10.1002/app.27091
Published online 20 September 2007 in Wiley InterScience (www.interscience.wiley.com).

ABSTRACT: Both viscoelastic behavior and plastic deformation in compression were investigated on new polythiourethane networks based on diisocyanates and tri- or tetra-thiols. Dynamic mechanical analysis was used to characterize the mechanically-active α and β relaxations as a function of crosslink density and nature of the diisocyanate. Data molecular analysis on these novel materials led to conclusions in good agreement with earlier statements on the well-known epoxy-amine networks. Besides, consideration of the relaxational behavior, and especially in the β relaxation region, allowed one to interpret the plastic deformation properties of the systems under study and to predict their poor resistance to fracture. By the way, analysis of the energy required to yield permitted determination of a new characteristic temperature, T_y, which can be compared to the thermomechanical main transition temperature, T_α, and to the glass transition temperature, T_g. © 2007 Wiley Periodicals, Inc. J Appl Polym Sci 107: 455–462, 2008

Key words: polythiourethane; dynamic mechanical analysis (DMA); crosslink density; secondary transition; plasticity

INTRODUCTION

Ophthalmic lenses have long been made of inorganic glass. However, the main innovation in last century was the replacement of inorganic glass by organic polymeric materials because of their lightness, good impact strength, moldability, processability, and dyeability. Unfortunately, the refractive index of conventional organic glasses is far below that of inorganic materials so that thicker lenses are required. Since the development in 1947 of the acrylic resin CR39 (diethylene glycol bis(allyl carbonate) of refractive index 1.49), many new materials have been designed to get high refractive index and low chromatic dispersion (high Abbe number). To increase the refractive index, atoms of high atomic number have been added in the chains, such as sulfur. Now, sulfur containing polythiourethanes are widely used as ophthalmic materials.[1–6] Whereas the chemical aspects of the polymerization are quite well-known,[7–10] very few mechanical and viscoelactic characterizations have been published on such materials.[11]

In this study, starting from a commercial formulation, the isocyanate and thiol components have been modified to permit molecular analysis of the mechanical properties at the molecular level. Our main goals are the following: (i) to establish a link between the structure of the polythiourethane networks and their viscoelastic properties, particularly by focusing on the mechanically-active relaxations observed both in the glass transition temperature range (α motions) and in the sub-T_g range (β motions associated with the secondary relaxation); (ii) to collect the stress–strain curves in compression mode to characterize the plastic deformation in the sub-T_g range; and (iii) to connect the yield and plastic flow properties to the relaxational behavior, as already reported before for various polymeric systems and especially for epoxy-amine networks (see a review article in Ref. 12).

EXPERIMENTAL

Materials

The polythiourethane networks were prepared by step polymerization of multifunctional thiols and isocyanates. Two diisocyanates, one trithiol, and one tetrathiol were used to vary the crosslink density and the properties of the synthesized networks. Their acronyms and chemical formulae are given in Table I. These chemicals were supplied by Mitsui Chemicals and then used without further purification. The nomenclature used is xNDI/nSH, with x the mass percentage of norbornane diisocyanate NDI

Correspondence to: J. L. Halary (jean-louis.halary@espci.fr).
Contract grant sponsor: Essilor International.

TABLE I
Monomers Used to Synthesize the Networks

Type	Acronym	Structure
Isocyanate	XDI	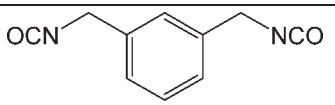
	NDI	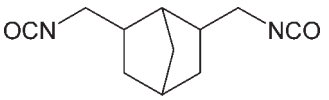
Thiol	3SH	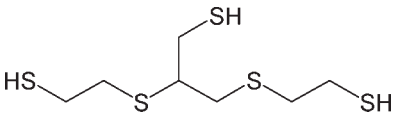
	4SH	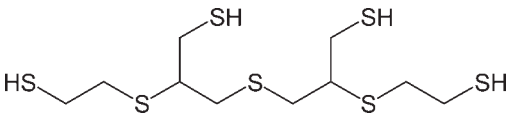
	2SH	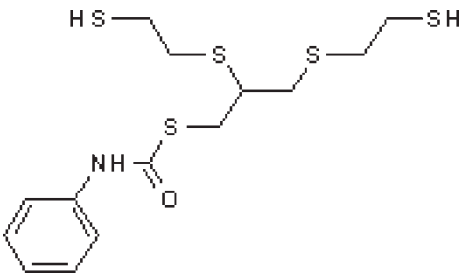

within the isocyanate blend (*m*-xylylene XDI/norbornane NDI), and *n* the functionality of the thiol (3SH or 4SH).

With the aim of enlarging the available range of crosslink density, the crosslinking agent 3SH was modified by reaction with phenylisocyanate into the dithiol 2SH (Table I) which acts as a chain lengthener. Then, mixtures of 3SH and 2SH containing variable amounts of 2SH were reacted with the diisocyanate XDI. The resulting networks (see again Table I) are coded 00NDI/2SH*y* with *y* the mass percentage of dithiol 2SH within the thiol blend (3SH/2SH).

Reactions were performed at a stoechiometric ratio $[SH]_0/[NCO]_0 = 1$, where $[SH]_0$ and $[NCO]_0$ are the initial concentrations of thiol —SH and isocyanate —NCO functions, respectively.

The curing cycle (Fig. 1) mimics the industrial conditions. It has been chosen to achieve a good structural homogeneity and, in turn, to prevent any distribution of refractive indices within the material. 0.01% of an organo-tin compound, dibutyultindichloride (DBTDCl), supplied by Aldrich, was used as the catalyst. Dibutyltin species, indeed, are known to complex the isocyantes by acting as Lewis acids.[13] To allow easy demolding, a demolding agent (0.1%

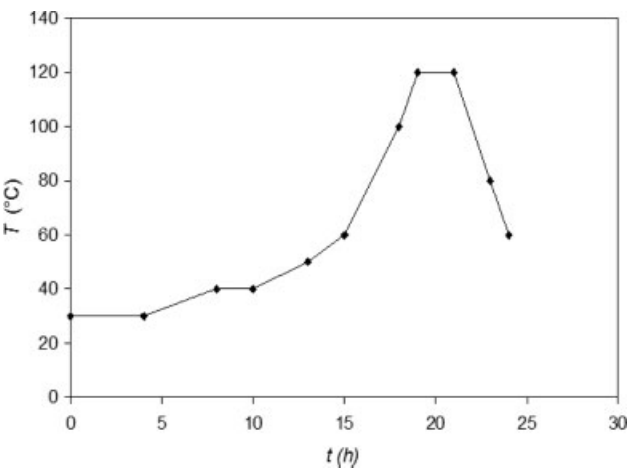

Figure 1 Cure cycle for the preparation of the networks.

TABLE II
Main Characteristics of the Networks Under Study

Network	ξ (mol kg^{-1})	Refractive index	T_g (°C)	T_α (°C)	T_y (°C)	T_β (°C)
00NDI/3SH	1.85	1.665	80	80	81	31
50NDI/3SH	1.80	1.644	85	94	96	30
00NDI/4SH	2.70	1.670	92	93	89	30
50NDI/4SH	2.62	1.649	110	112	108	30
00NDI/2SH50	0.90			65		20
00NDI/2SH75	0.45			59		16
00NDI/2SH100	0.00			54		12

Zelec UN©) was also added. The effect of such agents is not well known or documented[14,15] but their efficiency is very satisfactory. Some articles suggest that segregation occurs during the polymerization, making the demolding agent incompatible with the surface and then forming a lubricant layer. The catalyst was first dissolved in the isocyanate component and then the thiol component and the demolding agent were added. After filtration and degassing under vacuum for 30 min at cold temperature (ice bath), the mixture was cast into mold at room temperature. Samples were cured just after mixing.

The theoretical crosslink density, ξ, was calculated for each network from the monomer initial composition, as already proposed in earlier studies on epoxy networks.[16] The calculated crosslink densities are given in Table II. The crosslink points come from the thiols: each trithiol creates one crosslink point, each tetrathiol creates two crosslink points, and the presence of the chain lengthener 2SH leads to a drop of crosslink density.

When available, the refractive index values for the various networks under study are also reported, for information, in Table II.

Dynamic mechanical analysis

Dynamic mechanical analysis is probably the simplest technique for the identification of polymer mechanically-active relaxations. Its principles and applications can be found in recent review articles (see, for instance, Refs. 17,18). Let us just recall here that the dynamic modulus E^* can be split, at any temperature, into a in-phase elastic component E' and a $\frac{\pi}{2}$-dephased viscous component E'', whose under peak area is representative of the mechanical energy dissipated during the deformation at a given frequency.

Most of our thermomechanical measurements were carried out on fully cured samples using a rheometrics solid analyzer (RSA II) in three point bending geometry. Data were collected between −130 and 180°C at a heating rate of 2°C min^{-1} and a frequency of 1 Hz. The samples were parallelepipedic bars (2 × 10 × 48 mm^3). The same device was used to obtain the tensile dynamic mechanical spectrum and the modulus at the rubbery plateau at the same frequency and temperature ramp, using 1 × 3 × 30 mm^3 bars.

The multifrequency analysis was carried out on a TA Q800 device, used in single cantilever geometry and operated in isothermal conditions. Measurements were taken every 2.5°C with a 3 min isothermal stabilization. The samples used were 2 × 1 × 25 mm^3 bars. At each temperature, a frequency sweep was carried out from 0.1 to 32 Hz.

Multifrequency analysis permits determination of the apparent activation energy of the β transition. In the secondary relaxation range, master curves were built by following the frequency dependence of the temperature maximum, assuming an Arrhenian dependence of the transition. The temperatures T and T_0 are related to the corresponding test frequencies f and f_0 by the following relationship:

$$\ln\frac{f}{f_0} = \frac{E_a}{-R}\left(\frac{1}{T} - \frac{1}{T_0}\right) \quad (1)$$

The apparent activation enthalpy $\Delta H^{\neq}$ and entropy $\Delta S^{\neq}$ were calculated using the equations proposed by Starkweather:[19]

$$\Delta H^{\neq} = E_a - RT_0 \quad (2)$$

$$\Delta S^{\neq} = E_a - RT_0[1 + \ln(kT_0/2\pi h)] \quad (3)$$

where R, k and h represent respectively, the gas, Boltzmann's and Planck's constants and T_0 is the characteristic temperature relative to the reference frequency of 1 Hz.

Uniaxial compression tests

Uniaxial compression tests were carried out on a MTS 810 hydraulic testing system equipped with a temperature chamber. The samples used were parallelepipedic bars (3 × 3 × 6.5 mm^3). The deformation rate for the experiments was 2 × 10^{-3} s^{-1}. Stress–strain curves were collected at temperatures ranging

from −20 to 70°C. Before the tests, samples were stabilized at the chosen temperature for 30 min. The strain values involved in the experiments are quite small (typically less than $\varepsilon = 0.15$). Therefore, as a first approximation, changes in sample cross section can be ignored along the deformation and the engineering stress (ratio of the load to the initial cross section) can be regarded as identical to the true stress (ratio of the load to the actual cross section at given strain). Stresses given below are systematically the engineering stresses recorded on the computer of the testing system.

RESULTS AND DISCUSSION

Relaxational behavior

The typical shape of the dynamic mechanical spectra of the networks under study is shown in Figure 2, on the example of the sample 00NDI/3SH. Its inspection from the high to the lower temperatures reveals the occurrence of:

1. The main relaxation α, which is the mechanical expression of the glass transition phenomenon. It is characterized by an intense peak of the loss modulus E'' and by a decrease of E' by about two orders of magnitude.
2. A broad secondary relaxation β, whose E'' peak is centered around 30°C. Crossing of this relaxation is also marked by a decrease of E' by a factor of less than two.
3. Two other transitions around −50 and −100°C, visible on the E'' trace only. The latter has been ascribed to the motions of the —CH_2—CH_2— units coming from the thiols.[20] As these low temperature transitions correspond to very localized motions, they are not further discussed in the present article.

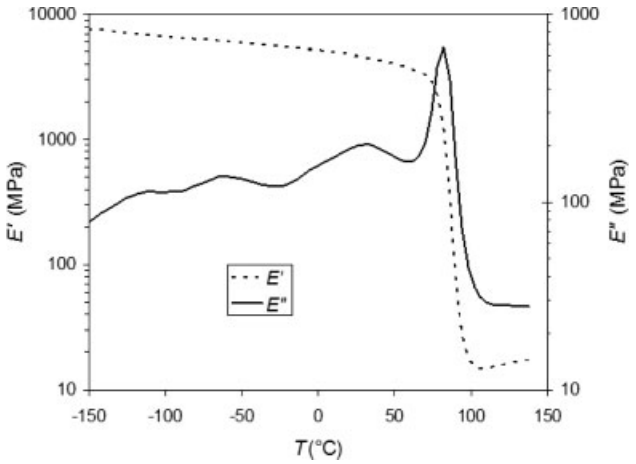

Figure 2 E' and E'' as a function of T, network 00NDI/3SH.

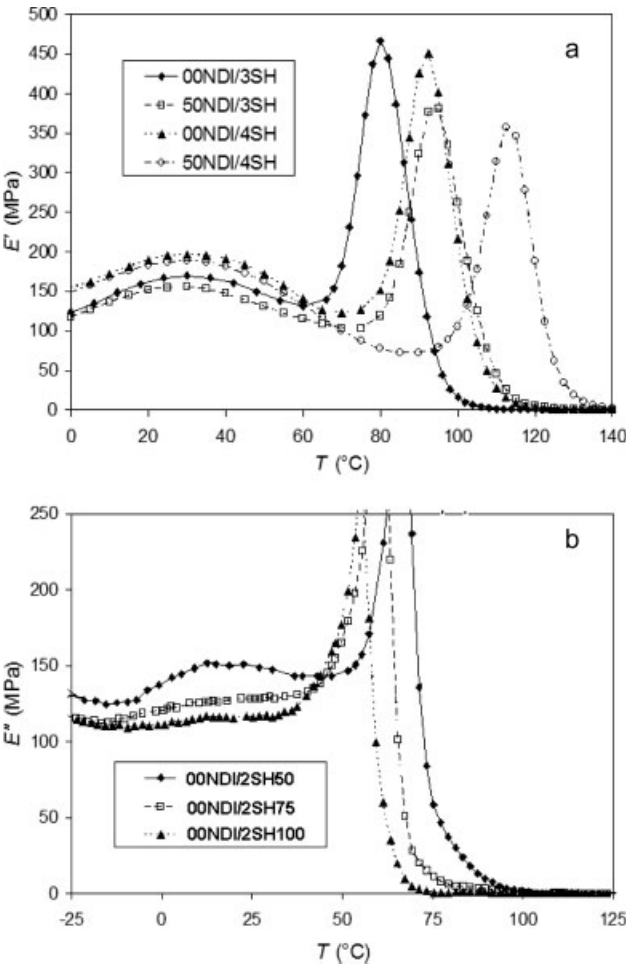

Figure 3 (a) E'' as a function of T for the networks xNDI/nSH (b) E'' as a function of T for the networks 00NDI/2SHy.

Let us concentrate first on the α relaxation, which can be analyzed from the data shown in Figure 3(a,b) relative to the xNDI/nSH and 00NDI/2SHy series, respectively. As shown in Table II, T_α values, taken as the temperatures of the maximum of the loss modulus E'' at 1 Hz, are in good agreement with the T_g values, determined from differential scanning calorimetry at a heating rate of 10°C min^{-1}.[21] Following the methodology proposed in previous studies,[16,22] it is convenient to interpret the T_α values by plotting T_α as a function of crosslink density (Fig. 4). In the 00NDI series, T_α (crosslinked) increases linearly with the crosslink density, ξ, irrespective of the details of thiol chemical formula. The corresponding equation is of the well-known form:

$$T_\alpha \text{ (cross linked)} = T_\alpha \text{ (uncross linked)} + K\xi \qquad (4)$$

where T_α (uncross linked) is the value of T_α relative to the sample 00NDI/2SH100 and K represents a constant.

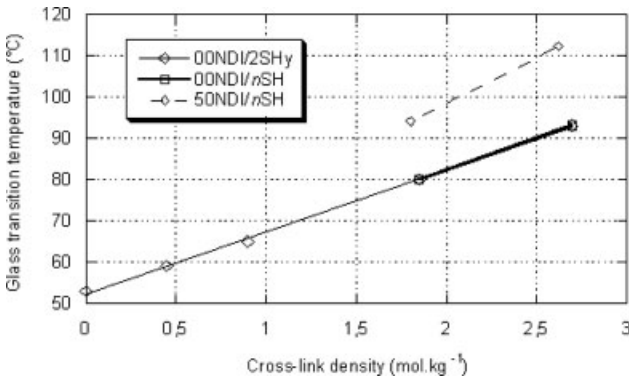

Figure 4 T_α (1 Hz) as a function of crosslink density for all the networks under study.

Because two samples only are available in the 50NDI series, we cannot prove the validity of eq. (4) in that case althrough it probably holds with a higher value of K as before. Anyway, at given ξ, it turns out that T_α is higher in the 50NDI series than in the 00NDI series. This is consistent with the fact that the NDI unit is much more bulky and rigid than XDI. This feature is also consistent with an higher value of K for the series 50NDI than for the series 00NDI, in agreement with previous findings for epoxy networks.[22]

Let us return now to Figure 3(a) and consider the β relaxation E'' peak in the xNDI/nSH series. The location of this broad peak on the temperature scale, and especially the value of its maximum, so called T_β, is unaffected by the type of isocyanate. This feature suggests that the cycles present in the isocyanate units of the network are not implicated in the secondary transition motions. In the same way, the type of thiol, SH3 or SH4, has no influence on the secondary transition temperature T_β. As the chemical structure of the two thiols is very similar, one can tentatively infer that the motions involved in the β process would be the same in both cases. Interestingly, the intensity of the relaxation is systematically higher with 4SH than with 3SH, a result compatible with the idea that the crosslinks are likely to participate in the β relaxation motions. By the way, one should mention that this idea is not novel: its validity was the key-point for elucidating the molecular origin of the β relaxation in model epoxy systems.[23]

At this stage, consideration of the networks prepared using the 2SH chain lenghtener [Fig. 3(b)] is useful to confirm the influence of the crosslinks on the propagation of the β-motions. Such materials, indeed, exhibit large changes in crosslink density (Table II).

It turns out that the β loss peak shifts to slightly lower temperatures with increasing 2SH content and that its intensity drastically drops. Whereas the former effect may have to do with the presence of new chemical units in the network chains, the latter provides clear evidence of the role of the crosslinks in the β relaxation process.

The multifrequency data allow the β transition to be characterized in more details. Figure 5(a) shows the plots of E'', measured at various frequencies, as a function of reciprocal temperature, assuming an Arrhenian dependence of the transition. These data are relative to the network 50NDI/4SH but it has been verified (data not shown)[21] that all the other xNDI/nSH networks behave the same. It is obvious from such data that a consistent master curve cannot be drawn. This gives evidence that several kinds of motions, each with its own activation energy and therefore with its own frequency dependence, are sampled under the broad β peak. By superimposing the maxima in the middle range of the transition, as shown in Figure 5(b), the apparent mean activation energy of the β relaxation can be determined. The values relative to the four xNDI/nSH networks available are given in Table III. They are roughly

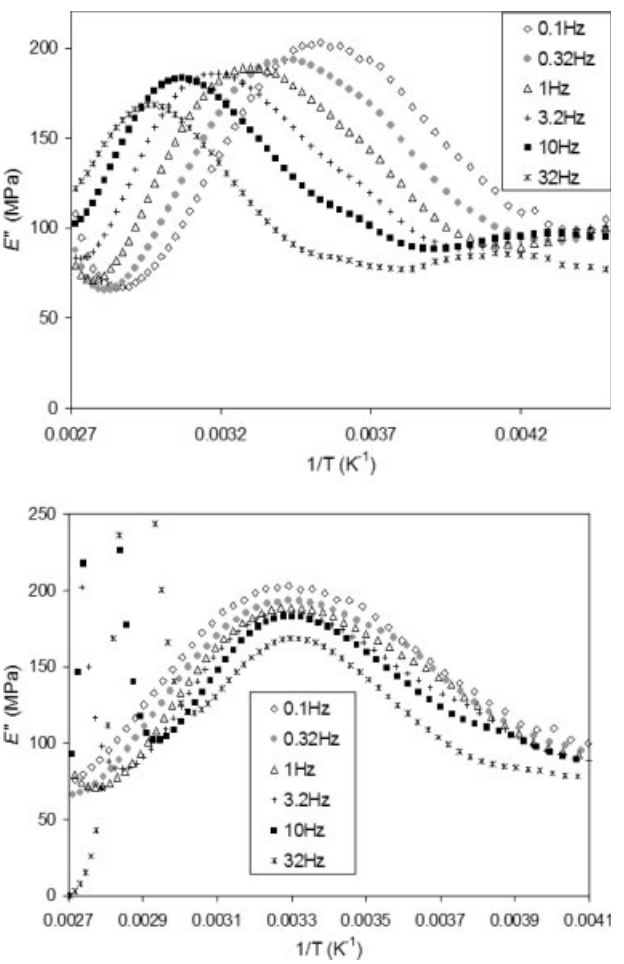

Figure 5 (a) Loss modulus E'' as a function of the reciprocal temperature, network 50NDI/4SH at different frequencies (b) Attempt to build a master curve on E'' as a function of reciprocal temperature, network 50NDI/4SH.

TABLE III
Apparent Activation Energy E_a and Entropy $\Delta S^{\neq}$ of the β Relaxation for the *x*NDI/*n*SH Networks

Network	E_a (kJ mol^{-1})	$\Delta S^{\neq}$ (J K^{-1} mol^{-1})
00NDI/3SH	93	68
50NDI/3SH	88	52
00NDI/4SH	99	89
50NDI/4SH	92	64

identical for all networks, corroborating the above conclusion that the same process is responsible for the β transition in each formulation. Use of the Starweather analysis [see eqs. (2) and (3)] also permits determination of the activation entropy $\Delta S^{\neq}$, which directly reflects the motion cooperativity. As recalled elsewhere,[19,23] low values of $\Delta S^{\neq}$ (less than 30 J K^{-1} mol^{-1}) are associated with very localized motions, while high values of $\Delta S^{\neq}$ (100 J K^{-1} mol^{-1} or so) concern cooperative motions, extending over a few repeat units. In the present case, values of $\Delta S^{\neq}$ are quite high (Table III) and their order of magnitude is the same as previously reported for epoxies.[22,24] As expected, replacing 3SH by 4SH and 50NDI by 00NDI favors high $\Delta S^{\neq}$values and, in turn, some cooperative character of the β motions. Indeed, the more crosslink materials presenting the more flexible units in between are the more likely to develop cooperative β motions.

Yielding properties

Figure 6 sketches the general shape of the stress–strain curves recorded for the materials under study. As mechanical testing has been carried out in compression mode, both stress and strain are negative quantities. They are conventionally presented here as positive, for sake of simplicity. All networks exhibit the same general behavior: namely, an initial linear evolution typical of the elastic response, then a curvature corresponding to the inelastic behavior before the yield point at maximum stress σ_y, and finally strain softening down to the plastic flow stress σ_{pf}.

On the molecular scale, plastic flow requires whole chain motions like those occurring above the α relaxation, whatever the considered temperature.[12] The suitability of this statement is validated in the present study by inspection of the plot of σ_{pf} as a function of $T - T_\alpha$ (Fig. 7): a unique master curve is obtained for all the samples, irrespective of the network chemical nature.

As far as the yield point is concerned, it is recognized[12] that it originates from conformational changes of the main chain, leading to an increase in high energy conformations corresponding to what would happen at a temperature above T_g. In the absence of β relaxation motions, such conformational changes can only occur in sites of lower local chain packing. As such sites are scarce, the price to pay for yielding is high or, in other words, σ_y takes a high value. In contrast, presence of efficient β motions induces quite a significant adaptation of the local surrounding of the mobile site, and therefore σ_y is likely to diminish. With this respect, the more cooperative the β motions, the more efficient they are and the less the value of σ_y is. With the *x*NDI/*n*SH networks, a change of slope is observed around the β transition temperature on the plots of σ_y versus temperature at constant strain rate (Fig. 8). This is indicative of the implication of the β-motions in the yielding process. In addition, it is worth noting, at any test temperature, that the lower values of σ_y concern the more crosslinked systems, that is, those prepared from the tetrathiol 4SH for which the β relaxation is the more pronounced.

A meaningful parameter can now be evaluated: the energy needed to initiate the plastic flow, *S*. As

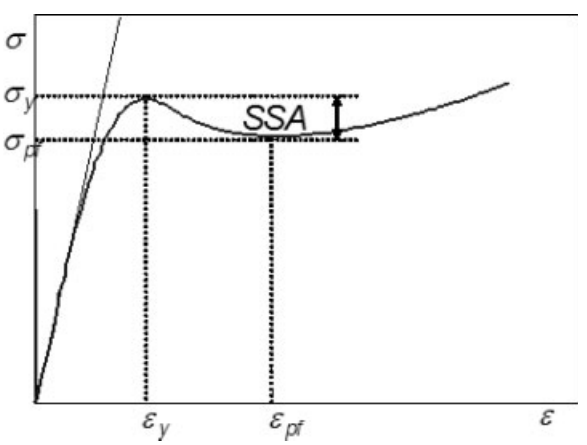

Figure 6 Scheme of a typical stress–strain curve and visualization of σ_y, σ_{pf}, and SSA.

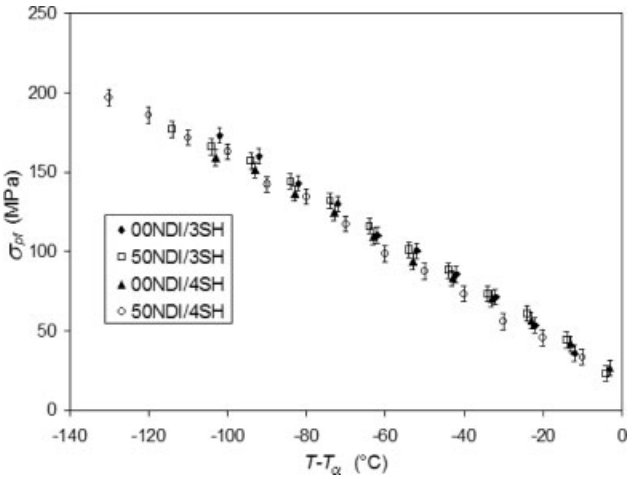

Figure 7 Plastic flow stress σ_{pf} as a function of $T - T_\alpha$ for the networks *x*NDI/*n*SH.

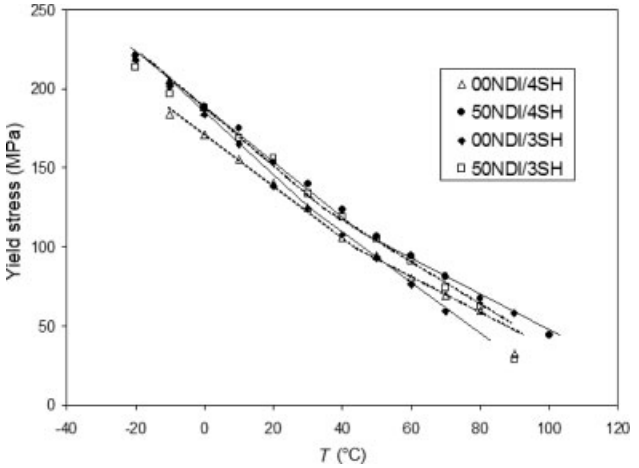

Figure 8 Yield stress σ_y as a function of temperature for the networks xNDI/nSH.

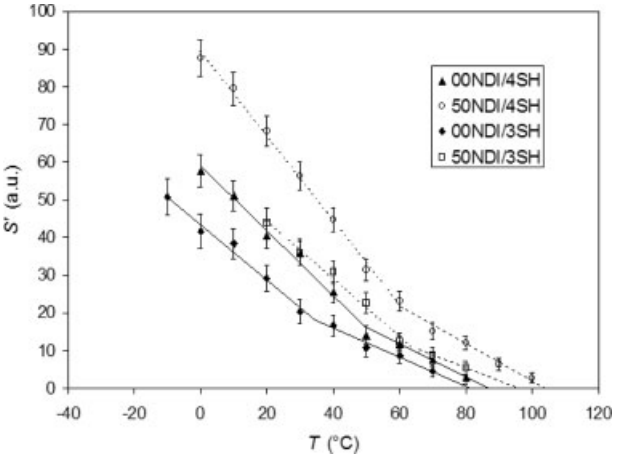

Figure 10 S' as a function of T for the networks xNDI/nSH.

sketched in Figure 9, it can be defined as the area under the stress–strain curve between the origin of coordinates and the yield point. As a matter of fact, this energy can be divided in two parts: a reversible elastic part, S_{el}, and an inelastic part, S'. Although consideration of S and S' yields about the same conclusions, it is convenient to focus on S′ and follow the temperature dependence of this quantity (Fig. 10). By extrapolation to 0, the curve S′-temperature yields the temperature, so called T_y, where no mechanical energy is needed to the material to start flowing. T_y is the mechanical analog of T_α (thermomechanically determined from DMA) or T_g (thermically determined from DSC). As can be seen from Table II, the agreement between these three quantities is quite satisfactory.

Figure 10 also shows changes of slope at temperatures close to the β-transition temperature, as a further argument in favor of the implication of the β-motions in the yielding process.

Quantitatively, the strain softening effect can be accounted for[12] by the strain softening amplitude SSA, defined as:

$$\mathrm{SSA} = \sigma_y - \sigma_{pf} \tag{5}$$

Since the plastic flow is linked to extended α motions and the yield point to α motions softened by β motions, high SSA is typical of highly decoupled α and β motions. On the other hand, low SSA indicates a strong coupling between α and β motions. In the studied materials (Fig. 11), SSA is quite high even approaching T_α, showing that β motions are not of great help for promoting plastic deformation. However, the 4SH-based materials have a lower SSA than the 3SH-based materials, in connection with the crosslink mobility.

Information can also be got[12] from the normalized strain softening amplitude nSSA, defined as:

$$\mathrm{nSSA} = \frac{\mathrm{SSA}}{\sigma_{pf}} = \frac{\sigma_y - \sigma_{pf}}{\sigma_{pf}} = \frac{\sigma_y}{\sigma_{pf}} - 1 \tag{6}$$

For the networks under study, nSSA is roughly a constant at low temperature (Fig. 12). A reasonable interpretation is that the crosslinks are immobilized and, as a consequence, that the ratio between the energies required to initiate yield point and plastic

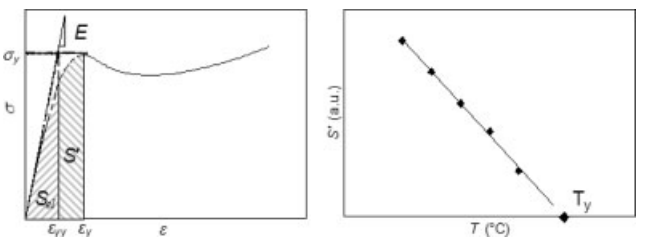

Figure 9 Scheme explaining the determination of S, S_{el}, S', and T_y.

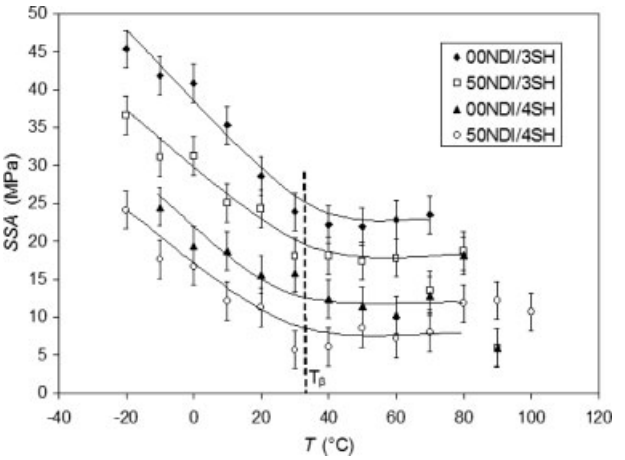

Figure 11 Strain softening amplitude SSA as a function of T.

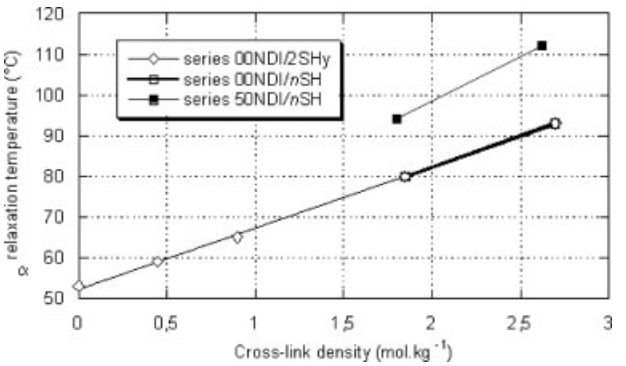

Figure 12 Normalized strain softening amplitude nSSA as a function of *T*.

flow motions is also a constant. Between T_β and T_α, the crosslinks become mobile, so that σ_y decreases faster than σ_{pf}: Therefore, nSSA increases (Fig. 12).

Finally, in the perspective of application of these thiourethane networks, it is useful to get an idea of their fracture properties. When studying the crack propagation,[21] all the materials have a stable brittle failure. The K_{Ic} values are quite low (from 0.6 to 0.9 MPa $m^{1/2}$) and typical of very brittle materials. This order of magnitude is what one may predict for rigid and highly crosslinked systems.

CONCLUSIONS

Polythiourethane networks for ophthalmic applications have been characterized by viscoelastic and mechanical testing. Following a strategy familiar to our laboratory,[12,22] formulations presenting progressive changes in chain mobility and crosslink density were investigated. Thus, it became possible to carry out a detailed analysis of the relaxational behavior of this new family of networks. A broad secondary transition was evidenced around room temperature and the activation energy analysis gave evidence for a succession of relaxation processes associated with multiple activation energies, and for significant motion cooperativity. In addition, the secondary relaxation motions were shown to spread over the crosslinks. All these features are identical to what has been previously reported for model epoxy-amine networks and can be interpreted in the same way.

Similarly, it was also possible to connect the yield and plastic flow properties to the relaxational behavior. By the way, analysis of the energy required to yield permitted determination of a new characteristic temperature, T_y, which is very close to the thermomechanical main transition temperature, T_α, and to the glass transition temperature, T_g.

The authors are indebted to Essilor International for the permission to publish. Thanks are also due to Dr L. Yean for his kind interest in this study.

References

1. Yean, L.; Brochu, C. Eur Pat Appl 408,459 A1 (1990).
2. Kanemura, Y.; Sasagawa, K.; Imai, M.; Suzuki, T. U.S. Pat. 5,087,758 (1992).
3. Zhu, Z.; Risch, B. G.; Yang, Z.; Lin, Y. N. U.S. Pat. 5,679,756 (1997).
4. Kosaka, M.; Kageyama, Y. U.S. Pat. 5,744,568 (1998).
5. Droger, N.; Halary, J. L.; Richard, G.; Rickwood, M.; Fr. Pat. 2,860,597 (2005); international extension 2006; 1,670,852.
6. Keita, G.; Obordo, J. O.; McClimans, P. A.; Turshani, Y. Y.; U.S. Pat. 6,887,401 (2005).
7. Choi, W.; Nakajima, M.; Sanda, F.; Endo, T. Macromol Chem Phys 1998, 199, 1909.
8. Nagai, A.; Miyagawa, T.; Kudo, H.; Endo, T. Macromolecules 2003, 36, 9335.
9. Nagai, D.; Sato, M.; Ochiai, B.; Endo, T. Macromolecules 2004, 37, 3523.
10. Nagai, A.; Ochiai, B.; Endo, T. Macromolecules 2004, 37, 7538.
11. Jaffrennou, B.; Droger, N.; Méchin, F.; Halary, J. L.; Pascault, J. P. e-Polymers 2005, 082.
12. Monnerie, L.; Halary, J. L.; Kausch, H. H. Adv Polym Sci 2005, 187, 215.
13. Reegen, S. L.; Frisch, K. C. J Polym Sci Part A-1 1970, 8, 2883.
14. Karbhari, V. M. J Mater Sci Lett 1998, 17 2061.
15. Serré, C.; Vayer, M.; Erre, R. J Mater Sci Lett 2001, 20, 1989.
16. Halary, J. L.; Bauchière, D.; Lee, P. L.; Monnerie, L. Polimery 1997, 42, 86 (Warsaw).
17. Menard, K. P. Dynamic Mechanical Analysis: An Introduction; CRC Press: Boca Raton, FL, 1999.
18. Menard, K. P. In Performance of Plastics; Brostow, W., Ed.; Hanser: Munich, 2000; Chapter 8.
19. Starkweather, H. W. Macromolecules 1981, 14, 1277.
20. Heijboer, J. In Molecular Basis of Transitions and Relaxations; Meier, D. J., Ed.; Gordon and Breach: New York, 1978.
21. Droger, N. Thesis of the University Pierre and Marie Curie (Paris VI), Paris, 30 September 2004.
22. Halary, J. L. High Perform Polym 2000, 38, 141.
23. Monnerie, L.; Lauprêtre, F.; Halary, J. L. Adv Polym Sci 2005, 187, 35.
24. Heux, L.; Halary, J. L.; Lauprêtre, F.; Monnerie, L. Polymer 1997, 38, 1767.